Proceedings of FEDSM2005
2005 ASME Fluids Engineering Division Summer Meeting and Exhibition
June 19-23, 2005, Houston, TX, USA

FEDSM2005-77251

CAVITATION EXPERIMENTS ON TURBOPUMP INDUCERS AND HYDROFOILS AT ALTA/CENTROSPAZIO: OVERVIEW AND FUTURE ACTIVITIES

Angelo Cervone
Project Manager, Alta S.p.A.
Via Gherardesca 5, 56121 Pisa, Italy

Cristina Bramanti
Project Engineer, Alta S.p.A.
Via Gherardesca 5, 56121 Pisa, Italy

Emilio Rapposelli
Senior Engineer, Alta S.p.A.
Via Gherardesca 5, 56121 Pisa, Italy

Luca d'Agostino
Professor, Dipartimento di Ingegneria Aerospaziale, Università di Pisa
Via G. Caruso, 56126 Pisa, Italy

ABSTRACT

The aim of the present paper is to provide some highlights about the most interesting experimental activities carried out during the years 2000-2004 through the CPRTF (Cavitating Pump Rotordynamic Test Facility) at Centrospazio/Alta S.p.A.

After a brief description of the facility, the experimental activities carried out on a NACA 0015 hydrofoil for the characterization of the pressure coefficient on the suction side and evaluation the cavity length and oscillations are presented. Then, the results obtained to characterize the performance and the cavitation instabilities on three different axial inducers are showed: in particular, a commercial three-bladed inducer, the four-bladed inducer installed in the LOX turbopump of the Ariane Vulcain MK1 rocket engine and the "FAST2", a two-bladed one manufactured by Avio S.p.A. using the criteria followed for the VINCI180 LOX inducer.

The most interesting results are related to the effects of the temperature on the cavitation instabilities on hydrofoils and inducers. Experiments showed that some instabilities, like the cloud cavitation on hydrofoils and the surge on inducers, are strongly affected by the temperature, while others seem not to be influenced by the thermal effects.

In the final part of this paper, some indications of the main experimental activities scheduled for the next future are provided.

INTRODUCTION

In space rockets turbopumps, used for propellant feeding, are a crucial component of all primary propulsion concepts powered by liquid propellant engines. Severe limitations are associated with the design of high power density, dynamically stable machines capable of meeting the extremely demanding suction, pumping and reliability requirements of space transportation systems (Stripling & Acosta [1]).

Cavitation, defined as "the formation of vapor bubbles in regions of low pressure within the flow field of a liquid" (Brennen [2]), is the major source of performance degradation of propellant feed turbopumps and also provides the necessary flow excitation and compliance for triggering dangerous rotordynamic and/or fluid mechanic instabilities of the machine (Sack & Nottage [3]; Natanzon et al. [4]; Braisted & Brennen [5]; Tsujimoto et al. [6]) or the entire propulsion system (POGO auto-oscillations, Rubin [7]). The recent fatigue failure of an inducer blade due to fluid dynamic instabilities of the LE-7 liquid Hydrogen turbopump and the consequent catastrophic loss of the rocket in November 1999 dramatically confirmed that the combined effects of rotordynamic fluid forces and cavitation represent the dominant fluid mechanical phenomena that adversely affect the dynamic stability and pumping performance of high power density turbopumps.

The cavitating performance of the inducers used for space propulsion systems, typically operating with cryogenic fluids such as liquid hydrogen and oxygen, is affected by the so-called thermal effects. These effects are caused by the temperature difference between the two phases that develops as a consequence of the latent heat of the evaporation/condensation phenomena caused by the volume changes of the cavities. In turn, this temperature difference modifies the vapor pressure in the cavities with respect to the unperturbed value corresponding to the bulk temperature of the liquid, thereby affecting the pressure differential that ultimately drives the dynamic response of the cavities. Therefore a local decrease of vapor pressure at the interface between the bubble and the fluid makes the bubble growth slower resulting in a better performance of the pump.

The scaling of the thermal effects, usually done using results obtained in hot water or in thermosensible fluids (such as Freon at room temperature), is not an easy and immediate result, and requires more than the usual techniques of dimensional analysis (Moore [8]). The impact of the thermal effects on the performance of pumps and inducers has been extensively investigated by the open literature (Fruman [9], Stahl & Stepanoff [10]); at the present day, on the other hand, the dependence of the cavitation-related instabilities on the temperature has not been sufficiently investigated.

As a rough initial approximation, the cavitating behavior of a rotating machine can be related to that of a static cascade of hydrofoils. In this view, the first step for understanding cavitation instabilities and thermodynamic scaling effects is typically represented by experimentation on test bodies in hydrodynamic tunnels. Cavitation instabilities on hydrofoils are generated by fluctuations of the cavitating region caused by the inherent unsteady nature of the flow and the interaction with the pertinent boundary conditions.

At the present time a number of aspects of unsteady flow phenomena in cavitating turbopumps and hydrofoils, including their connection with thermal cavitation effects, are still partially understood and imperfectly predicted by theoretical means alone. Technology progress in this field must therefore mostly rely on detailed experimentation on scaled models. To this purpose, in the year 2000 Centrospazio Space Research Labolatory/Alta S.p.A. has designed and set up the CPTF (Cavitating Pump Test Facility), intended for general-purpose experiments on cavitating/noncavitating turbopumps, and its upgraded version, the CPRTF (Cavitating Pump Rotordynamic Test Facility), which is especially dedicated to the investigation of rotordynamic fluid forces in forced vibration experiments with adjustable rotational and whirl speeds of the impeller (Rapposelli, Cervone & d'Agostino [11]). A Thermal Cavitation Tunnel (TCT) can also be installed on the suction line of the facility in order to conduct similarity and thermal cavitation experiments on hydrofoils and test bodies (Rapposelli, Cervone, Bramanti & d'Agostino [12]).

This paper is intended to present the characteristics of the experimental apparatus and to provide an overview of the most interesting results obtained by experimentation carried out on 2D hydrofoils and different rotating inducers. Finally, some indications will be outlined about the main experimental activities scheduled for the next future.

NOMENCLATURE

c	hydrofoil or inducer chord length
C_p	pressure coefficient on hydrofoil
f	frequency of oscillations
L_{cav}	cavity length on hydrofoil
p_{in}	hydrofoil or inducer upstream pressure
p_V	vapor pressure
Re	Reynolds number
r_H	inducer hub radius
r_T	inducer tip radius
s	inducer blade spacing
St	Strouhal number
T	freestream temperature
V	freestream velocity
α	hydrofoil incidence angle
β_T	inducer tip blade angle
ϕ	flow coefficient
ϕ_{ref}	reference (design) flow coefficient of the inducer
υ	kinematic viscosity
ρ	density
Ω	pump rotating speed
ψ	head coefficient
σ	cavitation number

EXPERIMENTAL APPARATUS

The Cavitating Pump Rotordynamic Test Facility (CPRTF, Figure 1) has been designed for experimental characterization of turbopumps in a wide variety of alternative configurations (axial, radial or mixed flow, with or without an inducer). The facility, operating in water at temperatures up to 90°C, is intended as a flexible apparatus that can readily be adapted to conduct experimental investigations on virtually any kind of fluid dynamic phenomena relevant to high performance turbopumps. The test section (Figure 2) is equipped with a rotating dynamometer, for the measurement of the forces and moments acting on the impeller, and with a mechanism for adjusting and rotating the eccentricity of the impeller axis in the range 0÷2 mm and ±3000 rpm. The inlet section, made in Plexiglas, is transparent in order to allow for the optical visualization of the cavitation on the inducer.

The water pressure at the inlet of the test section can be adjusted by means of an air bag, while the temperature regulation is obtained by a heat exchanger and an electrical resistance. A Silent Throttle Valve is used for the variation of the pump load.

Two electromagnetic flow meters, mounted on the suction and discharge lines of the water loop, provide measurement of the inlet and outlet flow rates. The inlet pressure is monitored by an absolute transducer mounted immediately upstream of the test section, while a differential transducer is used for measuring the pump pressure rise.

Figure 1. The Cavitating Pump Rotordynamic Test Facility (CPRTF).

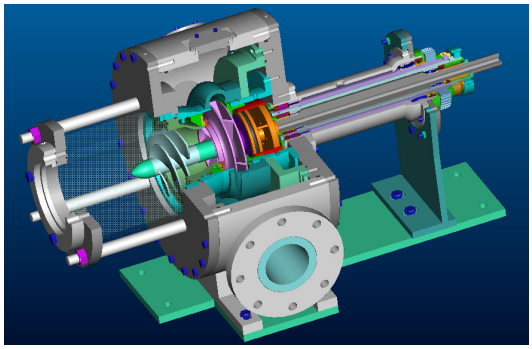

Figure 2. Cut-out drawing of the CPRTF test section.

In the experiments carried out to characterize the pressure fluctuations generated by the inducer, the transparent Plexiglas inlet section (Figure 3) is instrumented by several flush-mounted piezoelectric pressure transducers (PCB M112A22, ICP® voltage mode-type, 0.1% class) located at three axial stations: inducer inlet, outlet and at the middle of the axial chord of the blades. At each axial station at least two transducers have to be mounted with a given angular spacing, in order to cross-correlate their signals for coherence and phase analysis. As a result, waterfall plots of the power spectral density of the pressure fluctuations can be obtained as functions of the cavitation number $\sigma = (p_{in} - p_V)/(1/2)\rho\Omega^2 r_T^2$ in order to identify the presence of instabilities in the flow conditions under consideration. Cross-correlation of two pressure signals from different locations allows to determine the axial or azimuthal nature of each instability and, in the second case, the number of rotating cells involved.

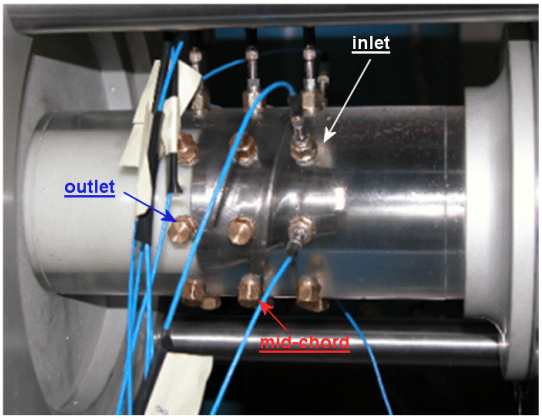

Figure 3. The transparent inlet section of the facility instrumented by piezoelectric pressure transducers.

The Thermal Cavitation Tunnel (TCT) configuration of the facility is specifically designed for analyzing 2D or 3D cavitating flows over test bodies. In this configuration the pump is simply used to generate the required mass flow.

The test body is mounted on a blind panel on the bottom of the rectangular test section (120x80x500mm, Figure 4). Optical access is allowed through three large Plexiglas windows located on the lateral and top sides of the test section.

The hydrofoil can be instrumented by several pressure taps, both on the suction side and on the pressure side. Three taps are located on the bottom panel upstream and 3 downstream of the test section to monitor the inlet/outlet pressure. The incidence angle can be manually adjusted as necessary for the specific experiment.

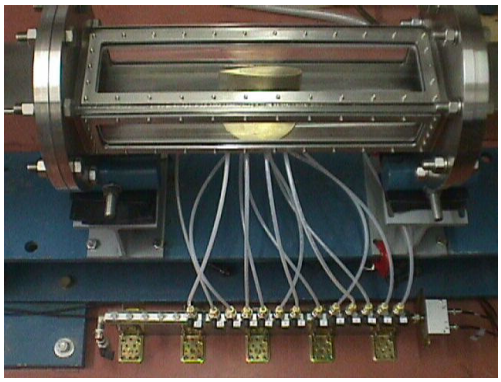

Figure 4. The test section of the Thermal Cavitation Tunnel.

In the following sections the most interesting results of the experimentation carried out in the facility during the last 4 years will be presented.

EXPERIMENTS ON HYDROFOILS

A set of experiments has been carried out in the Thermal Cavitation Tunnel on a NACA 0015 hydrofoil with 115 mm chord and 80 mm span length (Rapposelli, Cervone, Bramanti & d'Agostino [13]). Figure 5 shows a schematic of the test section, with the hydrofoil instrumented with 12 pressure taps, 10 on the suction side and 2 on the pressure side. In the presented experiments the hydrofoil inlet pressure has been measured by means of a flush-mounted absolute transducer, in order to avoid troubles related to the system frequency response.

The tunnel maximum velocity is 8 m/s and the Reynolds number ($\mathrm{Re} = c \cdot V / \upsilon$) has been maintained higher than $5 \cdot 10^5$ during the tests.

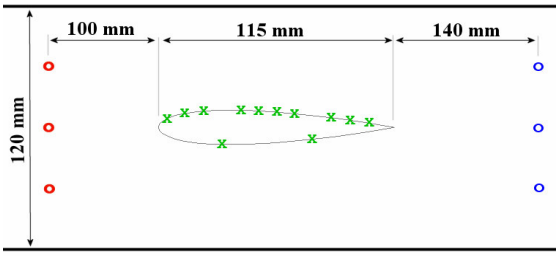

Figure 5. Schematic of the test section with the NACA 0015 hydrofoil and the locations of the pressure taps on the hydrofoil surface (x), at the section inlet (o) and outlet (o).

A first set of tests have been conducted to analyze the pressure coefficient in noncavitating and inertial/thermal cavitating conditions on the suction side of the hydrofoil. During these experiments, pressure was measured at each pressure tap for constant values of the tunnel velocity, water temperature, incidence angle and cavitation number $\sigma = (p_{in} - p_V)/(1/2)\rho V^2$.

In particular, Figure 6 shows the pressure coefficient profile in noncavitating conditions for different incidence angles at room water temperature. As expected, the experimental results are different from the surface pressure distribution in unconstrained flow: the lateral constraints to the flow pattern promote "solid blockage" with the increase of the dynamic pressure, the hydrofoil forces and moments at given incidence angle (Kubota, Kato & Yamaguchi [14]).

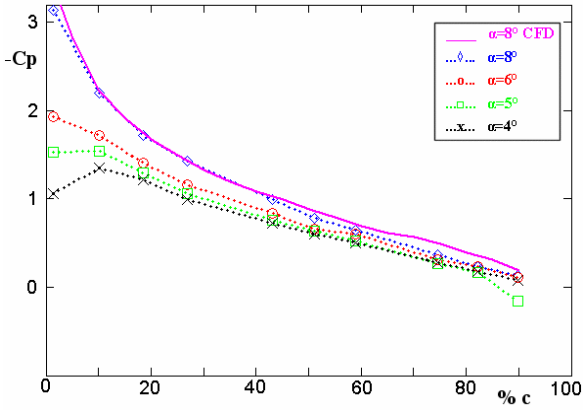

Figure 6. Pressure coefficient on the suction side of the NACA 0015 hydrofoil in noncavitating conditions for various incidence angles α at room water temperature. CFD simulation at 8° incidence angle and room water temperature (solid line). Experimental uncertainty in the evaluation of the pressure coefficient is about 1.5% of the nominal value.

Figure 7 compares the pressure profiles in cavitating conditions for three different freestream water temperatures at the same cavitation number and incidence angle. At higher temperatures the absorption of the latent heat at the cavity interface increases, reducing the vapor pressure under the unperturbed saturation value. This trend is well reflected in the figure: at 70 °C, due to pressure decrement under saturation value, the pressure recovery occurs more upstream than at room temperature.

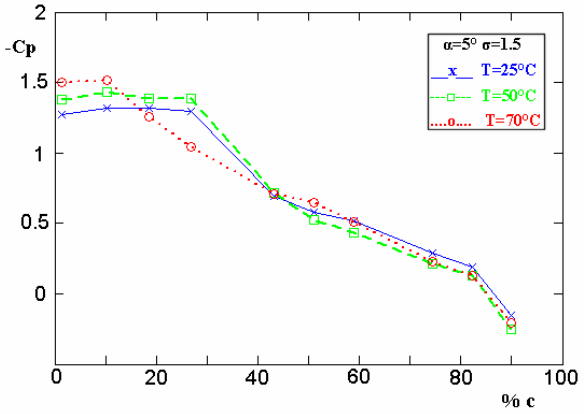

Figure 7. Influence of thermal cavitation effects on surface pressure distribution on the NACA 0015 hydrofoil at constant angle of attack α and cavitation number σ for several water temperatures T. Experimental uncertainty in the evaluation of the pressure coefficient is about 2% of the nominal value.

Other experiments have been carried out in order to determine the characteristics of the cavity length and oscillations at different incidence angles, cavitation numbers and freestream temperatures. Cavity length for each nominal condition was calculated by taking pictures of the cavitating hydrofoil at a frame rate of 30 fps, during a period of 1 second. Mean cavity length along the span was determined for each picture with a maximum estimated error of 4% of the chord length. As a final result of this process, maximum, minimum and mean value of the 30 cavity lengths were obtained. Figure 8 shows the maximum and minimum cavity lengths for various incidence angles at room water temperature. The cavity length and the frequency spectrum of the upstream pressure are shown in Figures 9 and 10 for the case of 8° incidence angle and room water temperature.

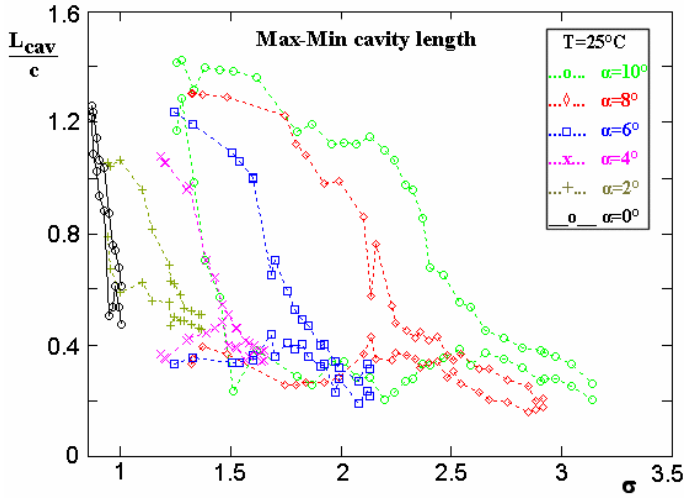

Figure 8. Normalized maximum and minimum lengths of the cavity as function of the cavitation number σ for various incidence angles α at room water temperature. Experimental uncertainty in the evaluation of the cavity length is about 4% of the chord length.

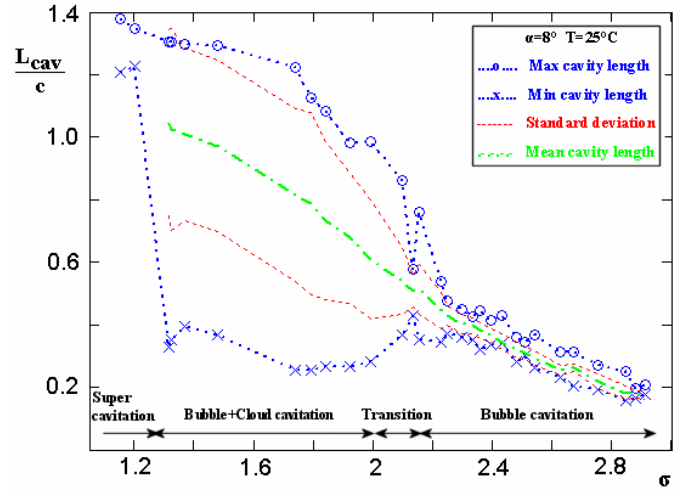

Figure 9. Characteristics of cavity length at 8° incidence angle and room water temperature. Experimental uncertainty in the evaluation of the cavity length is about 4% of the chord length.

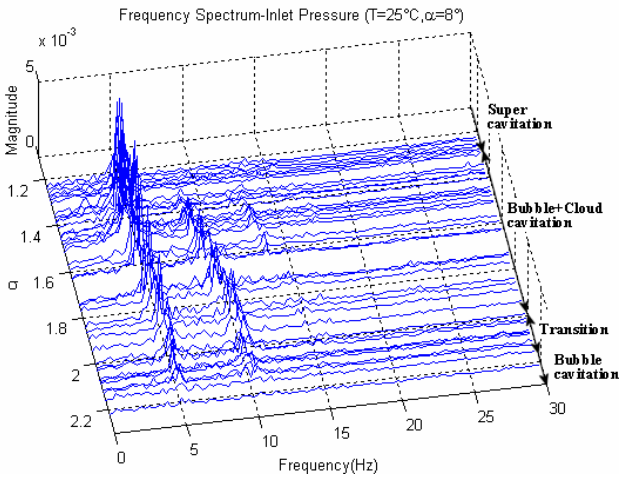

Figure 10. Frequency spectrum of the upstream pressure at 8° incidence angle and room water temperature.

Analysis of Figures 9 and 10 shows that the maximum and minimum cavity lengths provide a good qualitative indication of cavitation behavior on the hydrofoil at different cavitation numbers. Three different regimes of cavitation can be recognized, corresponding to different ranges of values of σ:

- Supercavitation (σ < 1.3): both minimum and maximum cavity lengths are larger than the chord length. There are practically no cavity oscillations and therefore the frequency spectrum tends to become flat.
- Bubble+Cloud cavitation (1.3<σ<2): the flow pictures show the occurrence of an initial zone of bubbly cavitation, followed by a second zone where the bubbles coalesce and strong cloud cavitation oscillations are observed. The frequency of these oscillations is almost constant at different cavitation numbers with a Strouhal number ($St = f \cdot c / V$) of about 0.2, similar to those obtained by Tsujimoto et al. [15] and Kjeldsen et al. [16].
- Bubble cavitation (σ>2.1): after a short transition zone, cloud cavitation disappears. Only the traveling bubble cavitation zone remains, with drastically reduced pressure oscillations (flat frequency spectrum).

Thermal cavitation tests were carried out with a similar procedure for 8° incidence angle at two different freestream temperatures (50 °C and 70 °C). Results are presented in Figure 11. The Figure shows that, at higher freestream temperatures, the "Bubble+Cloud cavitation" zone tends to spread over a wider range of cavitation numbers and to begin at higher values of σ, even if the frequency of the oscillations tends to remain the same. Similarly, supercavitation also begins at higher cavitation numbers. These findings seem to be in accordance with the results obtained by Kato et al. [17], who compared the temperature depressions in the cavity in water tests at 120 °C and 140 °C.

At higher freestream temperatures and constant cavitation number, the cavity tends to become thicker and longer, even when there are no oscillations. Cavitation at higher freestream temperatures looks quite different: bubbles are smaller and tend to coalesce more easily, resulting in a narrower and less defined "bubble zone" compared to the "cloud zone".

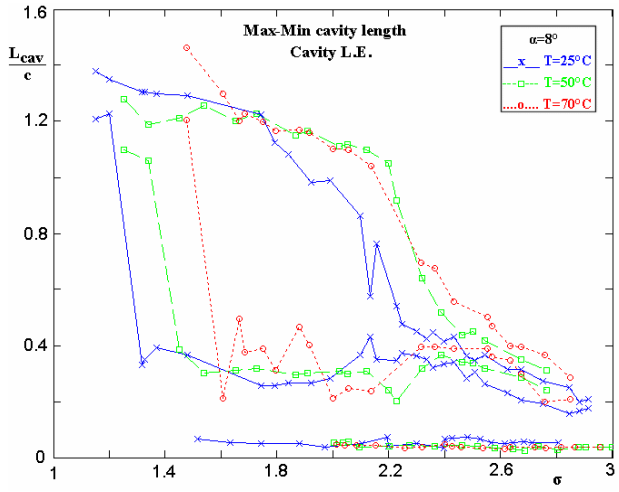

Figure 11. L.E., maximum and minimum lengths of the cavity for three different water temperatures T at 8° incidence angle. Experimental uncertainty in the evaluation of the cavity length is about 4% of the chord length.

The above results appeared significantly different from the typical data presented in the open literature, where at higher temperatures the cavitation breakdown tends to be shifted towards lower cavitation numbers and the cavity is shorter. A suitable explanation for this apparent disagreement can be given taking into account the influence of the lateral constraints: the observed increase of the cavitation thickness at higher temperatures, when the lateral wall is sufficiently near to the suction side, can promote cavity spreading along the longitudinal direction. This effect is more significant at higher incidence angles, for which the flow is forced to pass through a reduced cross section.

EXPERIMENTS ON AXIAL INDUCERS

In this section some results of the experiments carried out on three different axial inducers will be illustrated.

The first one is a 3-bladed, aluminum-made inducer of extremely simple helical geometry (Figure 12), having a tip radius $r_T = 81$ mm, a hub radius $r_H = 22.5$ mm, a tip blade angle $\beta_T = 9°$, a tip solidity $c/s = 3.05$ and 2 mm thick back-swept blades with blunt leading and trailing edges. It is manufactured by Fabbrica Italiana Pompe (FIP) S.p.A. for the food industry by welding the blades on the hub, and therefore it does not satisfy stringent geometric tolerances. The design flow coefficient of this inducer is $\phi = 0.06$.

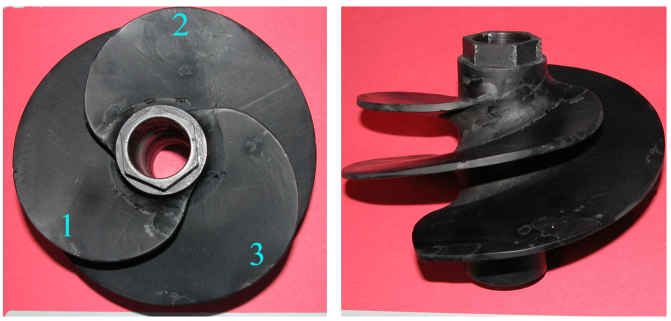

Figure 12. The FIP inducer.

The most interesting tests on the FIP inducer, related to the characterization of the cavitation instabilities, have been carried out mounting two piezoelectric transducers at each axial station of the Plexiglas inlet section (see Figure 3), with a relative angular spacing of 90°. A wide range of flow coefficients have been investigated: Figures 13 and 14 show the waterfall plots of the pressure fluctuation spectra measured at the inducer inlet section, for two different flow coefficients ϕ.

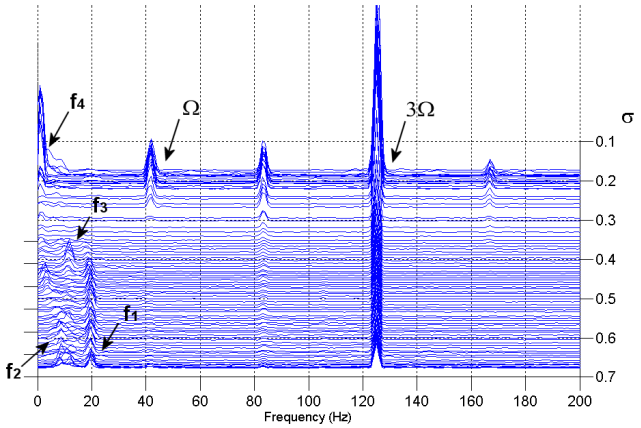

Figure 13. Waterfall plot of the power spectrum of the inlet pressure fluctuations in the FIP inducer at $\phi = 0.008$, 2500 rpm and room water temperature.

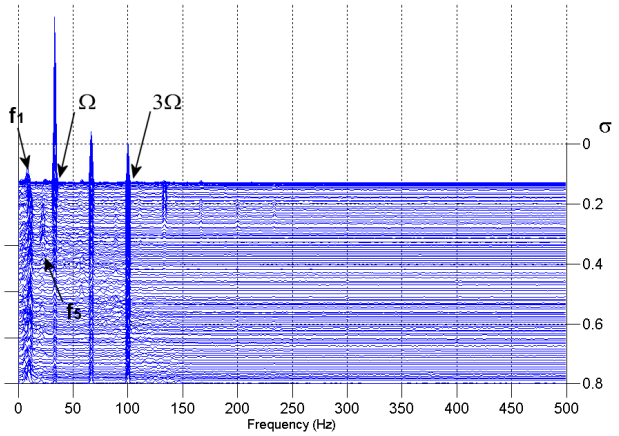

Figure 14. Waterfall plot of the power spectrum of the inlet pressure fluctuations in the FIP inducer at $\phi = 0.057$, 2000 rpm and room water temperature.

Analysis of the above spectra shows the occurrence of five forms of instabilities, denoted by frequencies from f_1 to f_5:

- The frequency f_1 is originated by a single-cell instability rotating in the circumpherential direction. This conclusion has been drawn by the cross-correlation analysis between the signals of the two piezoelectric transducers at the inlet station, which showed a phase delay of about 90° (equal to the angular spacing between the transducers). This instability, being subsynchronous, can probably be attributed to a form of rotating stall, whose occurrence is facilitated by the blunt shape and rough finishing of the blade leading edges. The oscillations appear for every value of the flow coefficient, with a frequency of about 0.34Ω that does not seem to depend on the presence of cavitation. A similar result, characterized by the detection of a rotating stall probably related to the occurrence of a strong backflow in the inducer inlet, has been reported by Uchiumi et al. [18] during the development of the LE-7A liquid hydrogen pump.

- The frequency f_2 is related to a 0-th order longitudinal instability, because the cross-correlation of the two pressure signals at the inlet station has a phase of 0°. This instability appears at all values of the flow coefficient with a frequency of about 9÷11 Hz, slightly dependent on the flow coefficient and very close to the expected noncavitating natural frequency of the facility: it is therefore most likely due to the excitation of the natural mode of oscillation of the flow in the inlet line of the inducer.

- The frequencies f_3 and f_4 are also due to longitudinal instabilities. The first is a typical cavitation auto-oscillation, whose frequency tends to decrease when the cavitation number is reduced (i.e., for more extensive cavitation). At the lowest values of the flow coefficient and the cavitation number this auto-oscillation leads to a surge (frequency f_4) characterized by strong axial oscillations at very low frequency (about 1 Hz).

- The frequency f_5 appears only at the highest values of the flow coefficient and for moderately low values of the cavitation number (just before the occurrence of the breakdown). It is a longitudinal instability, probably subsynchronous "cavitation surge", with a frequency of about 0.7Ω.

Experiments have been also carried out at elevated temperature ($T = 70\,°C$) in order to analyze the influence of the thermal cavitation effects on cavitation-induced instabilities. The results obtained for the same flow coefficients of Figures 13 and 14 are presented in Figures 15 and 16. The most significant differences are related to the flow instabilities occurring at frequencies f_4 and f_5: the strong oscillations caused by surge (frequency f_4) practically disappear at higher temperatures and lower flow coefficients, leading to a flatter spectrum at lower cavitation numbers, while "cavitation surge" oscillations (frequency f_5) also tend to become less intense at higher temperatures, moving towards higher values of the cavitation number. The frequency of the oscillations, however, does not seem to depend on the water temperature.

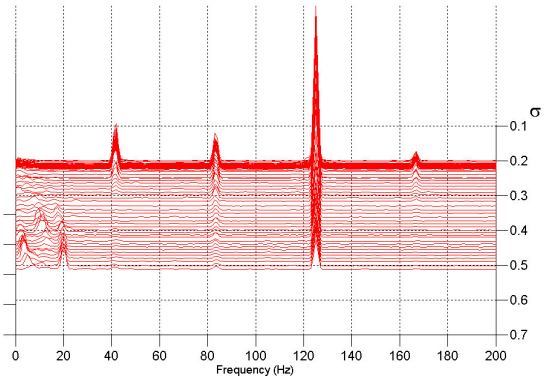

Figure 15. Waterfall plot of the power spectrum of the inlet pressure fluctuations in the FIP inducer at $\phi = 0.008$, 2500 rpm pump rotational speed and 70°C water temperature.

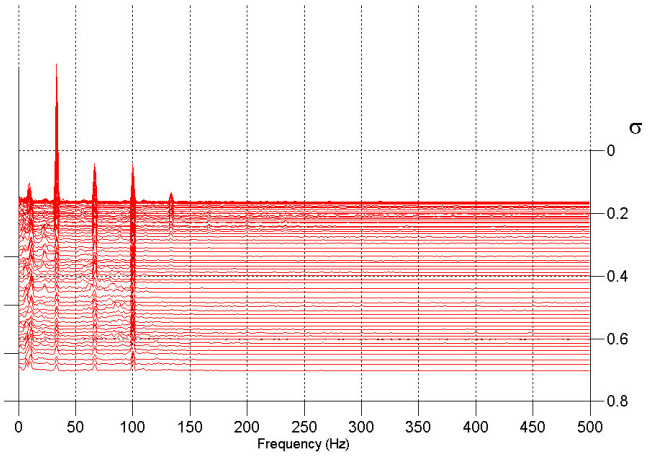

Figure 16. Waterfall plot of the power spectrum of the inlet pressure fluctuations in the FIP inducer at $\phi = 0.057$, 2000 rpm pump rotational speed and 70°C water temperature.

The second set of experiments is related to a prototype of the inducer manufactured by Avio S.p.A. and installed in the LOX turbopump of the Ariane Vulcain MK1 rocket engine (Figure 17). It is a four-bladed axial inducer made in Monel alloy, with a tip radius $r_T = 84$ mm, a profiled, variable-radius hub (36 mm inlet radius, 58 mm outlet radius) and backswept blades with sharp leading edges, variable thickness and nonuniform blade angle. The inlet tip blade angle is 7.7° and the tip solidity is 2.1.

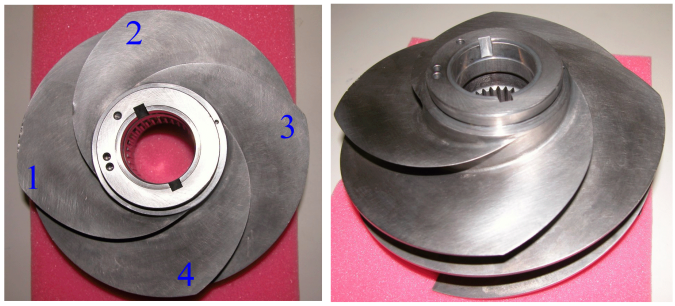

Figure 17. The MK1 inducer.

Some spectra of the pressure fluctuations measured on the MK1 inducer are presented in Figures 18, 19 and 20 and indicate that very few oscillation phenomena have been found. The observed instabilities are the natural mode of the facility at frequency f_2 (with some multiples, see Figure 18, probably due to non-linearity effects), an auto-oscillation (f_3) and a really smooth surge (f_4) with much less intense frequency peaks compared to those caused by the same phenomenon on the FIP inducer. At higher flow coefficients, near the nominal operating point of the MK1 inducer, the frequency spectrum becomes practically flat, except for the rotational frequency of the pump and its multiples (see Figure 20), thus confirming the effectiveness of the MK1 inducer design.

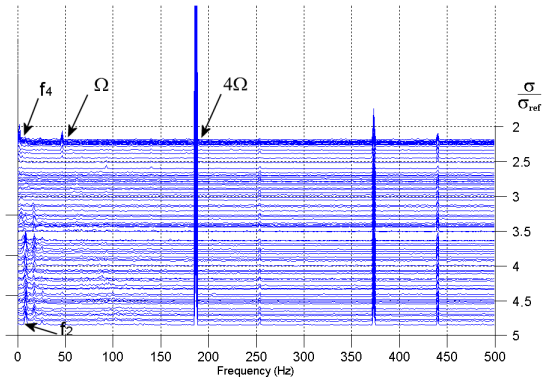

Figure 18. Waterfall plot of the power spectrum of the inlet pressure fluctuations in the MK1 inducer at $\phi/\phi_{ref} = 0.067$, 2800 rpm pump rotational speed and room water temperature.

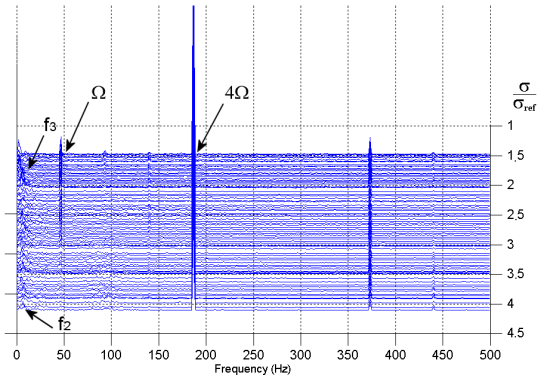

Figure 19. Waterfall plot of the power spectrum of the inlet pressure fluctuations in the MK1 inducer at $\phi/\phi_{ref} = 0.383$, 2800 rpm pump rotational speed and room water temperature.

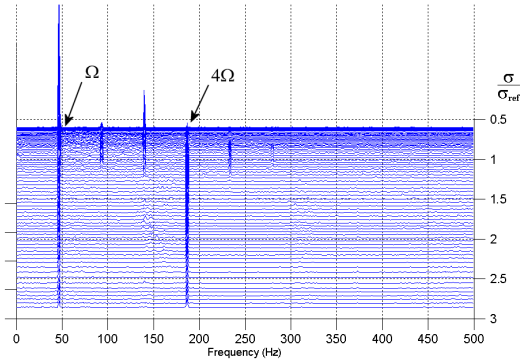

Figure 20. Waterfall plot of the power spectrum of the inlet pressure fluctuations in the MK1 inducer at $\phi/\phi_{ref} = 1.067$, 2800 rpm pump rotational speed and room water temperature.

The last set of experiments is referred to the FAST2 inducer (Figure 21), an axial pump manufactured by Avio S.p.A. using the criteria followed for the VINCI180 LOX inducer and experimentally validated in the CPRTF. The FAST2 is a two-bladed axial inducer, having a tip radius $r_T = 41.1$ mm, a profiled, variable-radius hub (15 mm inlet

radius, 28.3 mm outlet radius) and backswept blades with variable thickness and nonuniform blade angle. The inlet tip blade angle is about 7.5° and the tip solidity is 1.56. Figure 22 shows the cavitating performance of the FAST2 inducer at different flow coefficients.

Figure 21. The FAST2 inducer.

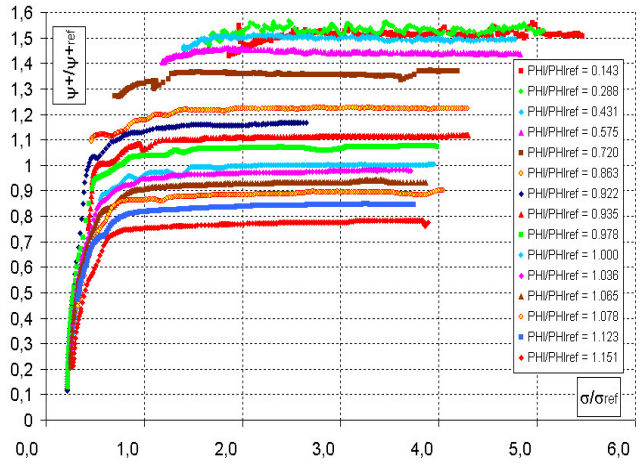

Figure 22. Cavitating performance of the FAST2 inducer. The head coefficient ψ/ψ_{ref} is plotted as a function of the cavitation number σ/σ_{ref} at room water temperature for $\Omega = 4000$ rpm and several values of the flow coefficient ϕ/ϕ_{ref}. Experimental uncertainty in the evaluation of the head coefficient is about 1% of the nominal value.

Figures 23 and 24 show the waterfall plots of the pressure fluctuation spectra measured at the inducer inlet section, for two different flow coefficients. The most interesting detected instabilities are:

- An auto-oscillation f_1, whose frequency is about 5÷12 Hz.
- A longitudinal instability f_2 at about 4.4Ω, with characteristics very similar to the higher order surge-mode instability recently observed by Tsujimoto and Semenov [19].
- A rotating phenomenon f_3 at a frequency of about 0.31Ω, coupled with a symmetrical one with respect to the rotational frequency of the inducer.

Figure 25 shows different levels of cavitation development on the FAST2 inducer, for a flow coefficient corresponding to its nominal operating point.

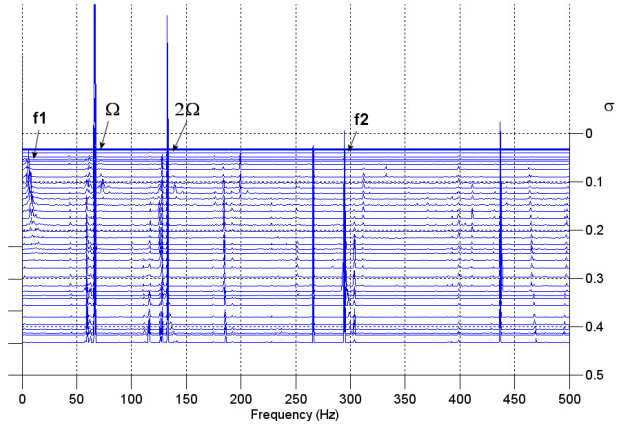

Figure 23. Waterfall plot of the power spectrum of the inlet pressure fluctuations in the FAST2 inducer at $\phi/\phi_{ref} = 1.216$, 4000 rpm pump rotational speed and room water temperature.

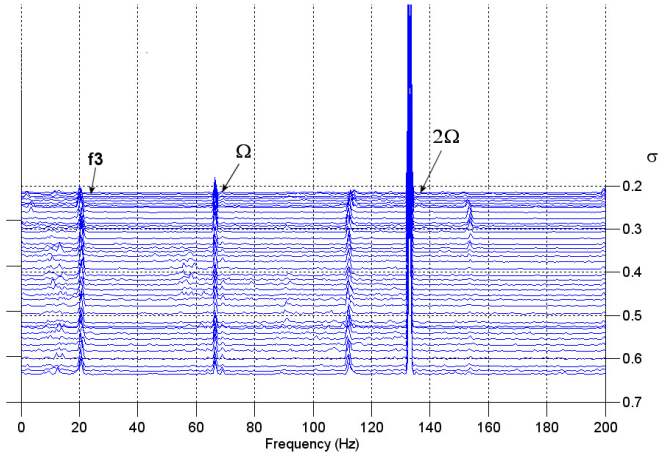

Figure 24. Waterfall plot of the power spectrum of the inlet pressure fluctuations in the FAST2 inducer at $\phi/\phi_{ref} = 0.135$, 4000 rpm pump rotational speed and room water temperature.

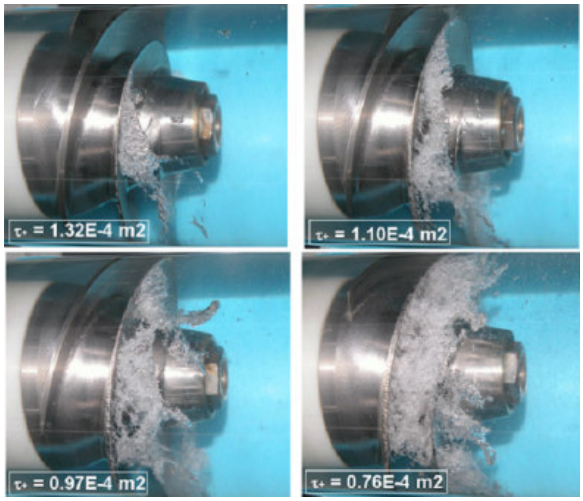

Figure 25. Development of cavitation on the FAST2 inducer in water at $Re = 1.24*10^6$. The flow conditions are: $\Omega = 3500$ rpm, $\phi/\phi_{ref} = 1$, room water temperature.

CONCLUSIONS

During the year 2000 Centrospazio Space Research Laboratory/Alta S.p.A. has designed and set up the Cavitating Pump Test Facility (CPTF). The facility and its upgraded configurations (the Cavitating Pump Rotordynamic Test Facility, CPRTF, and the Thermal Cavitation Tunnel, TCT), which use water as working fluid at temperatures up to 90°C, are flexible apparatus readily adaptable to carry out experimental investigations on virtually any kind of fluid dynamic phenomena relevant to hydrofoils and high performance turbopumps.

Some of the most interesting experimental campaigns carried out in the facility during the last years have been presented in this paper. In particular:

- A set of experiments in the Thermal Cavitation Tunnel on a NACA 0015 hydrofoil, for the characterization of the pressure coefficient on the suction side of the test body and the cavitation length. As expected, the pressure coefficient measurements showed that, in cavitating conditions, at higher temperatures the pressure recovery occurs more upstream than at room temperature. The characterization of the cavity length showed the occurrence of cloud cavitation oscillations that, at higher temperatures, tend to spread over a wider range of cavitation numbers and to begin at higher values of σ, even if the frequency of the oscillations tends to remain the same. This result, significantly different from the typical data presented in the open literature, is probably due to the influence of the lateral constraints: the increase of the cavitation thickness at higher temperatures, when the lateral wall is sufficiently near to the suction side, can promote cavity spreading along the longitudinal direction. This effect is more significant at higher incidence angles, for which the flow is forced to pass through a reduced cross section.
- Some experiments carried out on three axial inducers: the first is a three-bladed commercial axial pump (the so-called "FIP inducer"), while the other two have been used in space applications (the four-bladed inducer installed in the LOX turbopump of the Ariane Vulcain MK1 rocket engine and the "FAST2", a two-bladed one manufactured by Avio S.p.A. using the criteria followed for the VINCI180 inducer). The most interesting results have been obtained by the experiments for the characterization of the cavitation instabilities. On the FIP inducer rotating stall, auto-oscillation, surge, "cavitation surge" and the natural frequency of the facility have been detected. The MK1 frequency spectra showed auto-oscillation, a smooth surge at the facility natural frequency, with a practically flat frequency spectrum near its nominal operating point. The most interesting instability observed on the FAST2 inducer is a longitudinal one, at about 4.4 times the pump rotational frequency, with characteristics very similar to the higher order surge-mode instability recently observed by Tsujimoto and Semenov.

At higher temperatures the strong oscillations caused by surge practically disappear, while "cavitation surge" oscillations also tend to become less intense, moving towards higher values of the cavitation number. The frequency of the oscillations, however, does not seem to depend on the water temperature.

FUTURE TASKS

Several experimental activities are planned to be performed during the next years with the aim to completely exploit the capabilities of the facility. Some work is scheduled to improve the comprehension of the cavitation-induced flow instabilities and the influence of thermal effects on them, as well as to measure, by means of the rotating dynamometer, the unsteady rotor forces due to the presence of instabilities or to the imposition of a given whirl motion.

The Thermal Cavitation Tunnel will be used for experimentation on 2D cascades of hydrofoils, in order to validate analytical models currently under development. The cavity shedding effects leading to cloud cavitation oscillations need also to be studied in a more effective way, by both an analytical and an experimental point of view.

It should be interesting to carry out experiments in order to evaluate the transfer function of cavitating inducers, by adding to the facility an excitation and instantaneous flow measurements devices.

Inducers showing cavitation instabilities could be experimentally tested by a comparative point of view, in the CPRTF and in other similar facilities all over the world, in order to detect all the causes which originate such instabilities.

Finally, optical visualization of the cavitation on inducers and test bodies by means of a high-speed camera, coupled with the analysis of frequency spectra, could help to understand more about the instabilities detected during the experiments.

ACKNOWLEDGMENTS

The CPTF and CPRTF have been funded by the Agenzia Spaziale Italiana under the 1998 and 1999 contracts for fundamental research. The realization of the Thermal Cavitation Tunnel has been funded by ASI under the FAST2 program managed by the Centro Italiano Ricerche Aerospaziali. The authors would like to thank ing. Mauro Varetti of Avio S.p.A. for his kind assistance and express their gratitude to Profs. Mariano Andrenucci and Renzo Lazzeretti of the Dipartimento di Ingegneria Aerospaziale, Università di Pisa, Pisa, Italy, for their constant and friendly encouragement.

Finally, a special thank goes to all the persons who have given their precious collaboration to the design and the realization of the facility and to the experimental activities: Luisella Vigiani, Andrea Milani, Nicola Saggini, Renzo Testa and Lucio Torre.

REFERENCES

[1] Stripling L.B. and Acosta A.J., 1962, "Cavitation in Turbopumps – Part 1", ASME J. Basic Eng., Vol. 84, pp. 326-338.

[2] Brennen C.E., 1994, "Hydrodynamics of Pumps", *Concepts ETI, Inc*. and *Oxford University Press*.

[3] Sack L.E. and Nottage H.B., 1965, "System Oscillations Associated to Cavitating Inducers", ASME J. Basic Eng., Vol. 87, pp. 917-924.

[4] Natanzon M.S. el al., 1974, "Experimental Investigation of Cavitation Induced Oscillations of Helical Inducers", Fluid Mech. Soviet Res., Vol. 3 No. 1, pp.38-45.

[5] Braisted D.M. and Brennen C.E., 1980, "Auto-oscillation of Cavitating Inducers", *Polyphase Flow and Transport Technology*, ed. R.A. Bajura, ASME Publ., New York.

[6] Tsujimoto Y., Yoshida Y., Hashimoto T., 1997, "Observation of Oscillating Cavitation of an Inducers", ASME J. Fluids Eng.ing, Vol. 119, pp. 775-781.
[7] Rubin S., 1966, "Longitudinal Instability of Liquid Rockets Due to Propulsion Feedback (POGO)", J. of Spacecraft and Rockets. Vol. 3, No. 8, pp. 1188-1195.
[8] Moore R.D., 1970, "Prediction of Pump Cavitation Performance", NASA SP-304, *Symposium on Fluid Mechanics, Acoustic and Design of Turbomachinery*, Vol. II, Pennsylvania State University.
[9] Fruman D.H., 2002, "Review of thermal effects in the cavitation of inducers", *4th International Conference on Launcher Technology*, Liege, Belgium, December 3-6.
[10] Stahl H.A. and Stepanoff A.J., 1956, "Thermodynamics aspects of cavitation in centrifugal pumps", ASME J. Basic Eng., 87, 309.
[11] Rapposelli E., Cervone A. & d'Agostino L., 2002, "A New Cavitating Pump Rotordynamic Test Facility", *JPC, AIAA Joint Propulsion Conference and Exhibit*, Indianapolis, USA, July 7-10.
[12] Rapposelli E., Cervone A., Bramanti C. & d'Agostino L., 2002, "A New Cavitation Test Facility at Centrospazio", *4th International Conference on Launcher Technology*, Liege, Belgium, December 3-6.
[13] Rapposelli E., Cervone A., Bramanti C. & d'Agostino L., 2003, "Thermal Cavitation Experiments on a NACA 0015 Hydrofoil", *4th ASME_JSME Joint Fluids Engineering Conference*, Honolulu, Hawaii, USA, July 6-11.
[14] Kubota A., Kato H. & Yamaguchi H., 1992, "A new modelling of cavitating flows: a numerical study of unsteady cavitation on a hydrofoil section", *J. Fluid Mech.*, Vol. 240, pp. 59-96.
[15] Tsujimoto Y., Watanabe S. & Horiguchi H., 1998, "Linear Analyses of Cavitation Instabilities of Hydrofoils and Cascades", *Proc. of US-Japan Seminar: Abnormal Flow Phenomena in Turbomachinery*, Osaka, Japan, Nov. 1-6.
[16] Kjeldsen M., Effertz M. & Arndt R.E.A., 1998, "Investigation of Unsteady Cavitation Phenomena", *Proc. of US-Japan Seminar: Abnormal Flow Phenomena in Turbomachinery*, Osaka, Japan, Nov. 1-6.
[17] Kato H., Maeda M., Kamono H. & Yamaguchi H., 1996, "Temperature Depression in Cavity", *Fluids Engineering Division Conference*, San Diego, USA, July 7-11.
[18] Uchiumi M., Kamijo K., Hirata K., Konno A., Hashimoto T., Kobayashi S., 2002, "Improvement of Inlet Flow Characteristics of LE-7A Liquid Hydrogen Pump", AIAA Paper 2002-4161, 38th AIAA/ASME/SAE/ASEE Joint Propulsion Conference, Indianapolis, IN, USA, July 8-11.
[19] Tsujimoto Y., Semenov Y. A., 2002, "New Types of Cavitation Instabilities in Inducers", 4th Int. Conf. on Launcher Technology, Liege, Belgium, Dec. 3-6.

